

Article

Not peer-reviewed version

Further Development of a Low-Energy Arc-Ignition System for Nitrox/ABS Hybrid Propulsion Systems

[Stephen A. Whitmore](#)*, [Jared S. Coen](#), [Ryan J. Thibaudeau](#)

Posted Date: 11 March 2026

doi: 10.20944/preprints202603.0846.v1

Keywords: hybrid rocket; “green” propellants; nitrous oxide; 3-D printing; ignition latency



Preprints.org is a free multidisciplinary platform providing preprint service that is dedicated to making early versions of research outputs permanently available and citable. Preprints posted at Preprints.org appear in Web of Science, Crossref, Google Scholar, Scilit, Europe PMC.

Copyright: This open access article is published under a [Creative Commons CC BY 4.0 license](#), which permit the free download, distribution, and reuse, provided that the author and preprint are cited in any reuse.

Disclaimer/Publisher's Note: The statements, opinions, and data contained in all publications are solely those of the individual author(s) and contributor(s) and not of MDPI and/or the editor(s). MDPI and/or the editor(s) disclaim responsibility for any injury to people or property resulting from any ideas, methods, instructions, or products referred to in the content.

Article

Further Development of a Low-Energy Arc-Ignition System for Nitrox/ABS Hybrid Propulsion Systems

Stephen A. Whitmore *, Jared S. Coen and Ryan J. Thibaudeau

Mechanical and Aerospace Engineering Delt.; Utah State University, Logan UT, USA

* Correspondence: stephen.whitmore@usu.edu; Tel.: +1-(435)-797-2951

Abstract

Utah State University has developed a high-performance “green” hybrid propulsion technology based on the unique electrical breakdown properties of 3-D printed acrylonitrile butadiene styrene. Using 3-D printed ABS as fuel, typical startup sequences require approximately 5-15 joules; and once started, the system can be sequentially fired with no additional energy inputs required. The number of possible ignitions is limited only by the amount of fuel. The most technologically mature version uses gaseous oxygen (GOX) as oxidizer and 3-D printed ABS as fuel. While GOX is mass efficient, it lacks volumetric efficiency unless highly pressurized. Nitrox, a blend of GOX and nitrous oxide, improves propellant density and volumetric efficiency, while maintaining acceptable levels of mass efficiency (specific impulse). Nitrox can safely self-pressurize, eliminating the need for a separate oxidizer pressurization system and reducing overall complexity. However, using Nitrox as a direct replacement for GOX presents ignition decreases ignition reliably, significantly increasing cold-start ignition latency. This paper quantifies the latency, explores its sources, and analyzes expected behaviors. Solutions include raising combustion and storage pressures to boost oxygen content in Nitrox’s liquid phase and increasing combustion chamber pressure to reduce ignition delays.

Keywords: hybrid rocket; “green” propellants; nitrous oxide; 3-D printing; ignition latency

1. Introduction

Hybrid rocket systems are known for their safety and environmental benefits [1], making them a promising “green” alternative to hazardous propellants. They require only one fluid flow path and offer performance comparable to more complex bi-propellant liquid systems when optimized. Despite consideration for various applications, hybrids have not become mainstream in the space-launch and propulsion industries. By comparison, solid and liquid bi-propellant systems are far more developed, as hybrid technology remains immature.

As the Technology Readiness Level (TRL) rises, small-to-mid scale hybrid thrusters in the 25 to 250 N thrust range, are emerging as advanced, green propulsion options for both in-space and launch stage applications. Applications of hybrid rockets systems for upper stages of nano-launch vehicles due to their abilities to throttle, shut down, coast, and relight—capabilities that help offset increased dry mass over solid motors. These “smart-stages” can deliver payloads to orbit, enable precise orbital maneuvers, and support endo-atmospheric maneuvering for diverse defense uses. Hybrids are particularly appealing as a potential environmentally sustainable alternative to hydrazine; a propellant commonly used in spacecraft that is known for its significant toxicity and associated hazards. The commercial SmallSat market is prioritizing alternatives to hydrazine for in-space propulsion.

1.1. On the Restartability of Hybrid Rocket Systems

Historically, hybrid rockets have not been regarded as viable options for in-space propulsion, primarily because no dependable, non-pyrotechnic, reusable ignition method was available. While

hybrid rockets offer increased safety due to the inherent stability of their propellants, this same stability poses significant challenges for ignition. Effective ignition requires a source capable of delivering adequate heat to pyrolyze the solid fuel grain at the motor's head end, while also supplying enough residual energy to surpass the activation energy threshold of the propellants. Conventional solid-propellant ignition systems typically employ energetic materials configured as pyrotechnic or "squib" charges, which ignite a secondary solid-propellant motor whose high-enthalpy output triggers full motor combustion. High-energy devices also pose environmental and operational risks. Pyrotechnic charges are highly vulnerable to electromagnetic hazards (HERO, MIL-STD 464) and large charges are unsafe for many launches. Since most pyrotechnic ignitors are single-use, restartable hybrid propulsion systems have yet to be developed or deployed [2].

1.2. Three-Dimensional Printing as an Enabling Technology for a Low-Power Hybrid Arc Ignition System

The hybrid restart issue has been resolved by leveraging the electrical breakdown properties of certain thermoplastics printed using fused deposition manufacturing (FDM [3]). Few materials demonstrate these surface-arcing characteristics. Whitmore et al. [4] found that, among commercial feedstocks, acrylonitrile butadiene styrene (ABS) offers the best qualities for this application. Extruded ABS lacks suitable electrostatic breakdown properties, making 3-D printing necessary feature for this low-energy ignition process.

FDM-printed ABS, normally highly resistive, develops concentrated surface charges under a moderate electrostatic potential due to its layered structure [5]. These charge concentrations carve a conduction path, known as an arc-track, along the material surface, Hastings et al., [6], and Jiang et al. [7]. As shown in Figure 1, pyrolysis occurs when an inductive arc between electrodes embedded into the fuel material ablates hydrocarbon vapor along the fuel surface. Introducing oxidizing flow at oxygen partial pressures above two atmospheres ignites the pyrolyzed vapor through Joule heating.



Figure 1. Inductive Pyrolysis of 3-D Printed ABS Fuel.

The dielectric properties of FDM-printed ABS enabled the creation of a family of High-Performance Green Hybrid Propulsion (HPGHP) systems. A key PRL patent [8] features the low-power arc-ignition system using gaseous oxygen as oxidizer, requiring no more than 10W of power and only 3 joules per ignition [9]. Ignition count depends solely on fuel supply.

HPGHP has been engineered to achieve a high level of reliability. Prototypes with thrust from 0.5 N to 1500 N have been built and tested. Arc-ignition with GOX has been thoroughly tested at both ambient and vacuum conditions [10,11] at NASA Marshall Spaceflight Center (MSFC). Based on the

ground-test results of Ref. [10] a 10-N thruster with an additively manufactured fuel grain was designed, built, and flown from Wallops Flight Facility, reaching 172 km altitude and operating successfully five times under the hard-vacuum of space. Whitmore and Bulcher provide further details of this experiment [12].

In its most mature configuration, HPGHP relies on using gaseous oxygen (GOX) as the oxidizer. Unfortunately, for flight applications, using GOX is operationally infeasible. While GOX is a mass-efficient hybrid oxidizer, it is less efficient volumetrically, unless stored at very high pressures, due to its low specific gravity. Accordingly, there remains a need for a safe and efficient, alternative oxidizer with greater density.

1.3. Using Nitrous Oxide as an Alternative Hybrid Rocket Oxidizer

Nitrous Oxide (N_2O , [13]) is a cost-effective, widely available oxidizer that provides higher density compared to GOX. It has long been considered the “standard” oxidizer for hobby-rocket hybrid enthusiasts. In 2002, Scaled Composites LLC used a hybrid rocket with N_2O and hydroxyl terminated polybutadiene (HTPB) propellants to win the Ansari X-prize by carrying three people above the von-Karman line at 100 km altitude [14].

N_2O exists as a two-phase saturated liquid below its critical temperature of 36.4 °C. At room temperature (20 °C), its vapor pressure is about 5,050 kPa (732 psia) with a liquid density of 0.785 g/cm³. This density matches gaseous oxygen at around 59,800 kPa (8,670 psia), nearly 12 times higher than N_2O 's vapor pressure. Storing gaseous oxygen at such pressure requires *much* heavier tanks than for N_2O . Therefore, in flight systems, the lighter tank required for Nitrox compensates for its lower specific impulse compared to GOX.

1.3.1. Safety Concerns Associated with Using Pure Nitrous Oxide as a Hybrid Rocket Oxidizer

Pure liquid N_2O is considered non-toxic, non-explosive, and non-flammable by the US Occupational Safety and Health Administration, (OHSA, [15]) and USAF studies [16] show it is difficult to detonate in its liquid state. However, vapor-phase N_2O can release up to 1.87 MJ/kg of energy during decomposition, posing explosion risks due to increased gas volume. Its strong polarity makes it a good solvent, absorbing hydrocarbons or contaminants from tank liners or piping, which can catalyze dangerous decomposition reactions.

In flight applications, close coupling of the oxidizer tank and motor case increases the risk of contamination upstream of the thrust chamber. As N_2O is consumed, adiabatic cooling lowers tank vapor pressure, potentially enabling combustion instabilities to initiate backflow across the injector, causing hot hydrocarbon gases to enter oxidizer feed lines or the tank, potentially leading to runaway N_2O decomposition reactions. Several accidents have resulted from such events. The 2007 Scaled Composite's accident resulted from contaminated nitrous oxide ignited by an electrostatic spark. Reference [18] presents a summary of nine verified accidents related to inadvertent, uncontrolled nitrous oxide decomposition events.

1.3.2. Using Nitrox as an Inherently Safe, Higher-Density, Alternative to Pure Nitrous Oxide

Fortunately, adhering to procedures established by the medical and dental anesthesia fields [17] significantly lessens this decomposition risk. “Nitrox,” a two-phase mixture of N_2O and GOX as used for propulsion applications is created in a similar manner to laughing gas, but with lesser GOX mass-concentrations. Much like making soda water with dissolved carbon dioxide, Nitrox is produced by bubbling pressurized oxygen gas into liquid nitrous oxide until saturation is achieved. The dissolved oxygen replaces much of the nitrous oxide vapor in the tank's ullage space, greatly lowering the chance of a decomposition reaction and enabling safe handling of nitrous oxide in clinical settings. Karabeyoglu [18] and Whitmore [19] qualitatively assess the lowered risks achieved by replacing N_2O with Nitrox.

Preliminary PRL tests using Nytrox [20,21] show that Nytrox, has the potential to replace GOX as an efficient, higher density, alternative that is significantly safer to use the N_2O . Conservative theoretical calculations predict that the Nytrox/ABS combination has the potential to exceed a vacuum specific impulse (I_{sp}) of 300 seconds—substantially higher than what is achievable with hydrazine. Moreover, Nytrox can safely self-pressurize, eliminating the need for a separate, volumetrically inefficient oxidizer pressurization system and thereby significantly reducing overall system design complexity.

1.3.3. Arc-Ignition Reliability and Latency Issues Associated with Using Nytrox as a Hybrid Rocket Oxidizer

As described by Refs. [19,22], a primary issue associated with using Nytrox as a hybrid oxidizer is a decrease in ignition reliability and a significant increase in the cold-start ignition latency, using the arc-ignition system. The authors of Ref. [19] addressed reliability and latency problems in ignition by implementing a GOX “prelead.” In this approach, gaseous oxygen was used to fill the piping beyond the run valve before testing began. When the run valve was opened, the Nytrox solution pushed the gaseous oxygen ahead of itself, enabling the arc-ignition system to work much like earlier HPGHP systems that used pure GOX as the oxidizer. Although this approach enabled the initial Nytrox development tests to move forward, it is not suitable for flight use. Using separate oxidizers for ignition (GOX) and operation (Nytrox) would make the system much more complex and considerably increase its overall weight.

A preliminary study (Ref. [22]) on Nytrox-hybrid arc ignition indicated that increased Nytrox ignition latency is associated with factors such as run tank temperature, pressure, oxygen content, and operating chamber pressure; however, the precise mechanisms remain unconfirmed. Elevated temperatures were observed to lower oxygen concentrations, thereby delaying ignition. The authors proposed that maintaining Nytrox at lower temperatures could decrease ignition latency. Additionally, they noted that employing a single-port injector intended for gaseous oxidizers may contribute to ignition delays and suggested that redesigning the system with multiple ports and enhanced mixing capabilities may offer improvements.

The study found that a thorough understanding of Nytrox ignition latency is still needed and recommended making this a focus for future research. Once this issue is fully understood, results from further testing could lead to engineering methods that minimize or eliminate Nytrox ignition delays. Addressing ignition latency is essential for the Nytrox HPGHP system—a technology with the potential to disrupt the market—to become fully functional. The following sections presents results from this follow-up test and development effort.

2. Materials and Methods

This section details the hardware and test procedures that were used to perform the follow ignition studies. The original studies of Refs. [19–22] employed the small legacy 12 N thruster system that was previously used for MSFC vacuum testing campaign of Ref. [10]. The initial thruster operated with oxidizer mass flow rates below 6 g/sec. To enable more robust ignition testing, a custom system was built to provide ten times greater thrust and mass flow. This section covers the thrust chamber design, outlines the rocket test infrastructure, and details the hot-fire data collection procedures. The final subsections detail the process for how the Nytrox solution is prepared for test firings.

2.1. Test Systems Hardware

This section describes the test systems hard used to perform the Nytrox ignition testing. The thrust chamber design is presented first, followed by a discussion of the arc-ignition system electronics. Finally, the hot-fire test support systems are described.

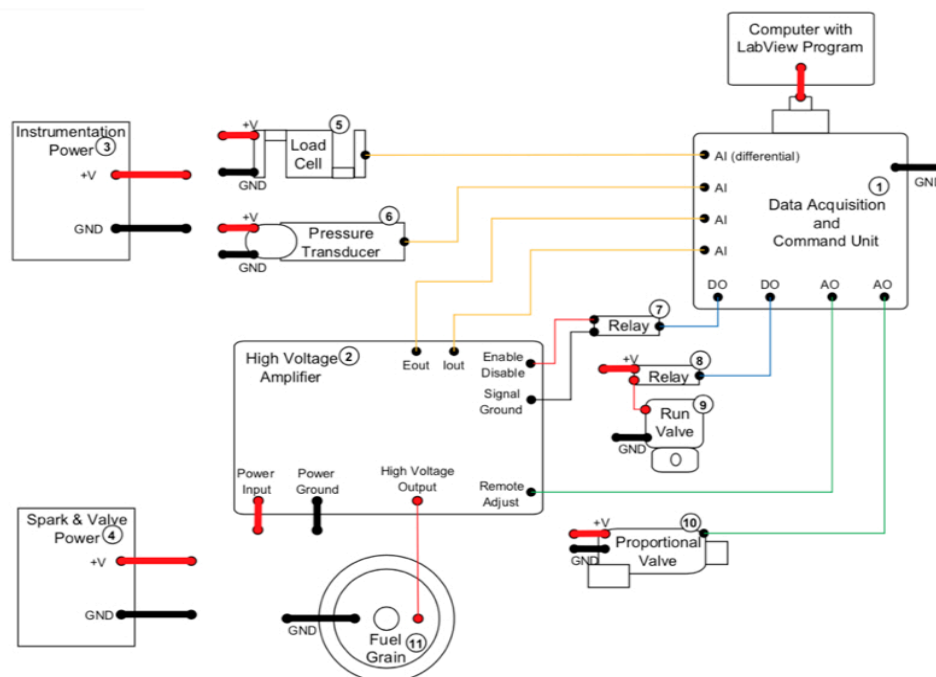


Figure 3. Motor Ignition System Electronics Layout.

2.1.3. Motor Test Support Systems

Figure 4 presents the piping and instrumentation diagram (P&ID) for the test systems. The stand measures oxidizer flow using a Venturi meter, thrust with a load cell, and monitors chamber and feed pressures as well as various temperatures via thermocouples placed along the flow path. A three-way valve enables rapid switching between Nitrox and GOX as oxidizers. The pressure-actuated oxidizer run valve located behind the combustion chamber is controlled remotely, whereas feed pressures are set manually to achieve the desired chamber conditions. Custom software manages consistent testing procedures, and data from the motor instrumentation pallet is transferred to the control laptop through USB. All tests took place in the PRL Ballistics and Survivability Limits Testing (BLAST) Lab at USU; further information can be found in Whitmore et al. (2020, [26]). Figure 5 displays the thrust chamber mounted on the test stand, ready for firing.

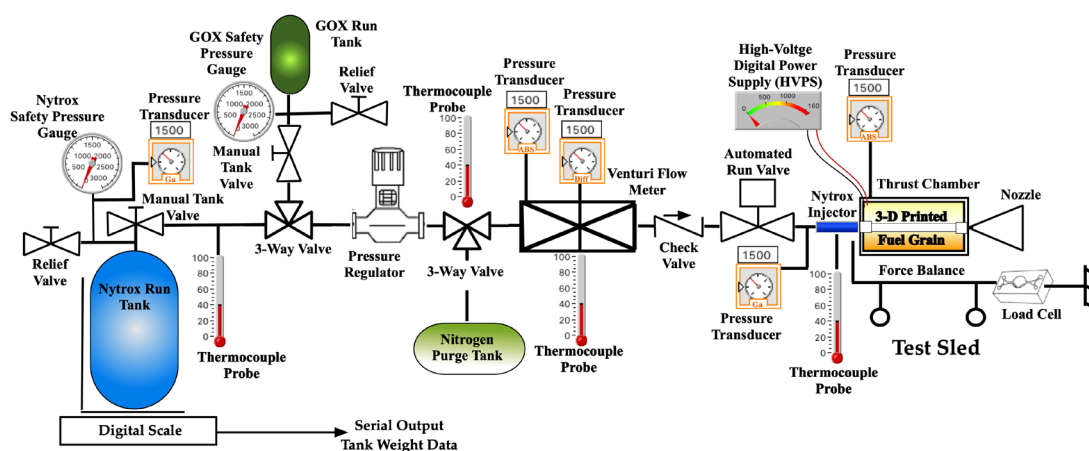


Figure 4. Piping and Instrumentation Diagram Showing Motor Test-Support Systems.

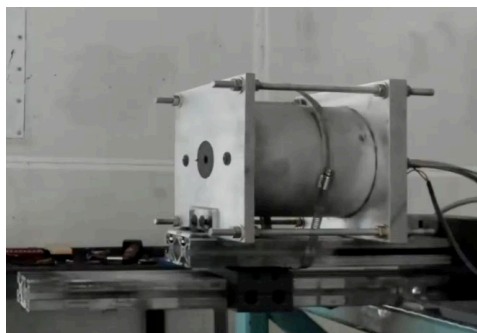


Figure 5. Thrust Chamber Mounted on Test Stand, Ready for Firing.

2.2. Test Procedures

The testing campaign began with an initial Nytrox tests that used a GOX pre-lead to confirm system functionality and determine minimum ignition latency. After establishing this latency, subsequent tests used only Nytrox. During GOX pre-lead runs, the Nytrox valve stayed closed while GOX was routed through the system and purged via quick cycling. The process then switched to Nytrox for ignition testing.

Each test used the same ignition sequence, with all commands automated and sent by a control computer. For the Nytrox series, burn times ranged from as short as 4 seconds to over 20 seconds. Before every test, the upstream regulator feed pressure was manually adjusted to achieve the targeted chamber pressure and thrust. Prior to opening the run valve, the fuel-pyrolysis process was triggered by powering the fuel grain electrodes through the HVPS one second in advance. After this 1-second spark lead, the run valve opened, beginning the measurement of ignition latency. To ensure ignition, the spark remained active for 2 seconds after the valve opened. Because ignition typically required less than 5 watts of power, there was no attempt to reduce or optimize the spark duration or overlap for these tests. Following each burn, an automated nitrogen (N_2) gas purge extinguished the combustion chamber flame.

A commercial Holley Nitrous Oxide Systems (NOS[®]) storage tank, as listed by the Holley catalog (2020, [27]), served as the nitrous oxide run tank. To replicate realistic operating conditions during hot-fire testing, the Nytrox tank—initially kept at $-15\text{ }^{\circ}\text{C}$ —was gradually warmed to ambient temperature during the tests. The tank was positioned on a digital scale, which provided real-time readings of the instantaneous tank mass throughout the burn.

Manual measurements were taken before and after the test, including the weight of the fuel grain, and the diameters of the fuel port at both the head and nozzle ends. The diameters of the nozzle throat and exit plane were also recorded. Additionally, the starting weight, pressure, and temperature of the oxidizer run tank were measured. All results were entered into a spreadsheet for later analysis.

2.3. Making the Nytrox Solution

Figure 6 illustrates the Nytrox percolation apparatus. The run tank is filled with N_2O , attached to a GOX supply, and GOX bubbles through the liquid nitrous oxide via a dip tube. The dip tube enables percolation and direct delivery of liquid Nytrox for hot fire tests. Oxygen dissolves in the liquid N_2O and carries nitrous oxide droplets into the gas phase, gradually reducing the liquid volume until vapor-liquid equilibrium is achieved.

To ensure consistent results, prior to filling the NOS[®] tank is chilled to $-10\text{ }^{\circ}\text{C}$ in an industrial-grade freezer while the N_2O service tank remains at room temperature. This temperature difference creates a pressure gradient for effective fluid transfer between tanks. For Nytrox manufacturing, the NOS[®] run tank is filled with nitrous oxide (typically 5 kg), the N_2O valve is closed, and the GOX valve opened to allow controlled flow into the run tank. The GOX regulator sets the final tank pressure. As

GOX enters, the tank weight increases until saturation is reached at the set pressure, enabling explicit control of the O_2 mass fraction in the run tank.

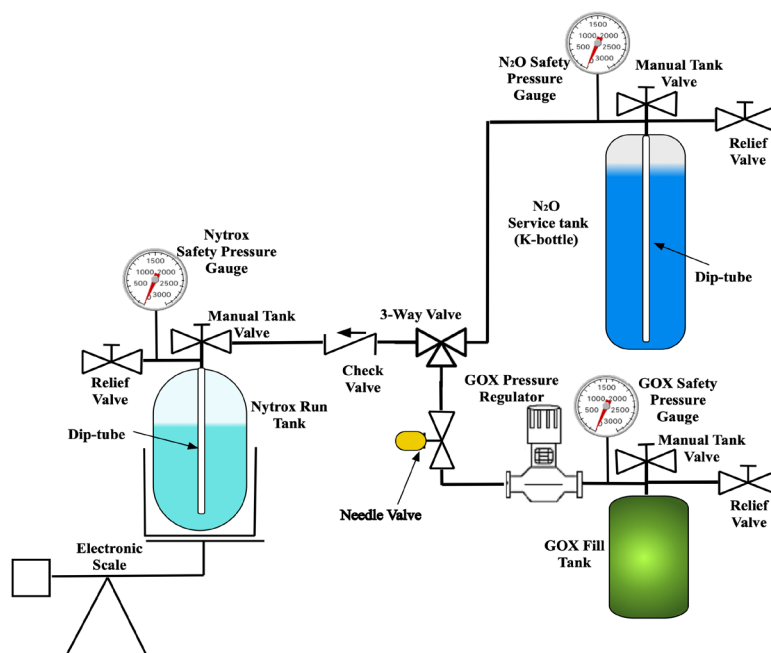


Figure 6. Schematic of the Nytrox Solution Perculation Apparatus.

3. Results

This section summarizes the main results of the Nytrox testing campaign, beginning with a GOX prelead Nytrox/ABS ignition test to verify system functionality and determine the minimum expected ignition response time. After the GOX prelead verification burn, fourteen Nytrox-only ignition tests were conducted with chamber pressure adjustments performed by manually adjusting the regulator set pressure. The section presents results from both test types, along with example time history and data summary plots.

3.1. Gox Prelead Time Tests

For this test, the nozzle throat diameter was approximately 0.26 in. (6.25 mm), and the expansion ratio was approximately 3.4:1. The injector set pressure was approximately 600 psig. Figure 7 plots the time history results from the first GOX prelead test. Plotted are (a) Thrust as measured by the test stand load cell, and as calculated from chamber pressure using the 1-dimensional de Laval flow equations (Anderson, [28], Chapter 4) and the known nozzle geometry. For this calculation the exhaust plume thermodynamic and transport properties were calculated using the NASA's Chemical Equilibrium with Applications (CEA) program [29,30]. CEA, developed at NASA Glenn Research Center, is an industry standard software package for calculating chemical equilibrium compositions and thermodynamic properties of mixtures. CEA can also determine theoretical rocket performance parameters like thrust, specific impulse, and characteristic velocity.

Additional Plots include (b) and overlay of the injector feed pressure and the resulting chamber pressure, (c) total, oxidizer, and fuel mass flow rates, (d) specific impulse values calculated using the data of Figures 7(a) and (c), nozzle exit pressure, and (f) consumed ignition power. As anticipated, during this initial test the motor ignited nearly instantaneously. The ignition delay, measured from the first response in injector pressure to the peak rise in chamber pressure, was approximately 130 milliseconds. Consumed ignition power was very low, less than 3.2 watts RMS.

It must be noted that Figure 7(d) shows the specific impulse to be rather low, just over 200 sec. Since Figure 7(e) shows the nozzle exit pressure closely matches ambient pressure, confirming

optimal expansion; the low specific impulse is likely due to the low mean chamber pressure of around 200 psia (1380 kPa). With this motor setup the lower operating pressure results in a fuel-rich oxidizer-to-fuel ratio, approximately 2.0; a value that lies well below the optimal 4.25–4.5 O/F ratio predicted for Nytrox/ABS combustion. (Ref. 19)

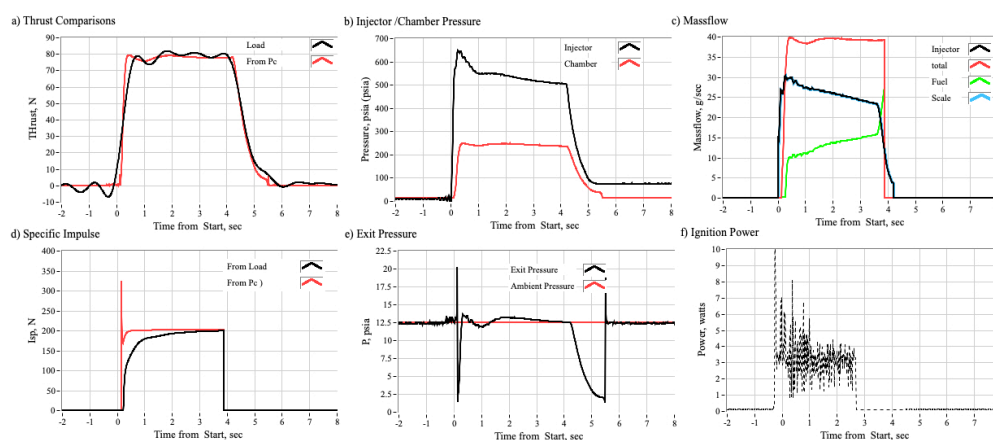


Figure 7. Time History Plots of GOX Prelead Ignition Test.

3.2. Nytrox-Only Ignition Tests

By manually adjusting the regulator set pressure, the 14 Nytrox ignition tests proceeded from low to high chamber pressure values. Across this data set, steady-state operating chamber pressure from approximately 80 psia (520 kPa) to 415 psia (2860 kPa) were achieved. During these tests the O_2 percentage in Nytrox was also varied by adjusting tank storage pressure, reflecting changes in O_2 solubility in N_2O due to pressure and temperature. Details of this solubility process are covered in the Results Section, 3.3.1 of this paper.

3.2.1. Time History Plots

Figure 8 presents the time history data from an initial low-pressure ignition test conducted at the lowest regulator pressure setting, approximately 200 psig. The parameters displayed correspond to those shown in Figure 7. For this experiment, the nozzle throat diameter was about 0.2 inches (5.1 mm), and the expansion ratio was close to 5:1. Under these conditions, the steady-state operating chamber pressure reached only around 80 psig. Additionally, compared with the GOX prelead data from Figure 7, the ignition delay was significantly longer, with the burn requiring nearly 2,100 milliseconds to attain the peak rate of pressure increase. The thrust profile exhibited values close to the lower detection limit of the test stand's load measurement system; consequently, the time history profiles presented in Figure 7(a) display a notable degree of noise. The specific impulse value was notably low, less than 100 seconds, primarily due to the over-expanded nozzle (refer to Figure 7e) coupled with the reduced operating pressure. Consistent with Figure 7, the mean ignition power remained low, registering below 2 watts.

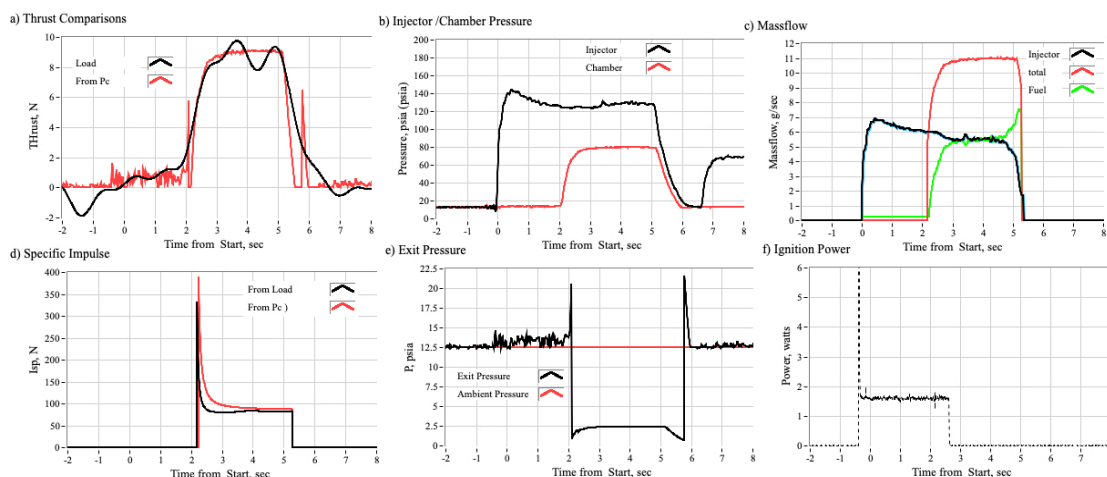


Figure 8. Time History Plots of Low-Pressure (80 psia) Nitrox Ignition Test.

Figure 9 presents time history data from a longer burn at a higher regulator setting of ~600 psig. The nozzle throat diameter was 0.2 inches (5.1 mm), with an expansion ratio near 5:1. The chamber pressure reached just over 400 psia, about five times higher than in Figure 8. Ignition delay was 300 msec—longer than the GOX prelead test's 130 msec, but shorter than for tests at very low chamber pressure. At this higher chamber pressure, the specific impulse reaches about 235 seconds, much higher than in the GOX prelead test performed at roughly half the steady-state operating pressure.

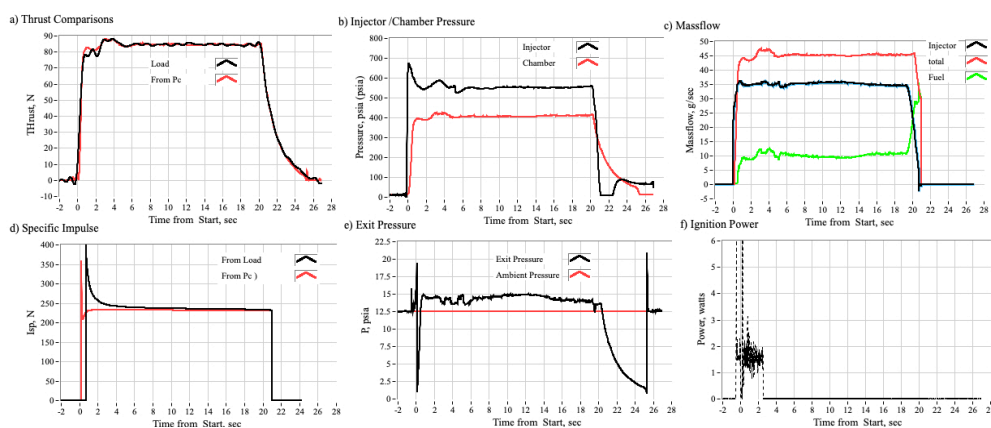


Figure 9. Time History Plots of High-Pressure (400 psia) Nitrox Ignition Test.

3.2.2. Exhaust Plume Images

Figure 10 compares exhaust plume images captured at the median steady-state burn time, corresponding to the data illustrated in Figures 8 and 9. In the low-pressure ignition test, Figure 10(a), the exhaust plume appears notably sooty and exhibits a smoldering characteristic. In contrast, during the high-pressure ignition test shown in Figure 10(b), the exhaust plume appears bright, distinct, and completely expanded, signifying that full combustion was achieved. Figure 10(a) demonstrates that ignition was only marginally achieved at this low pressure, suggesting that the chamber pressure threshold for successful nitrox ignition in this motor configuration is likely within the range of approximately 50–80 psia.

(a) Low Pressure Burn (Fig. 8) Exhaust Plume



(b) High Pressure Burn (Fig. 9) Exhaust Plume



Figure 10. Exhaust Plume Images for Low Pressure (Figure 8) and High Pressure (Figure 9) Nytrox Ignition Tests.

3.3. Ignition Test Summary Plots

This section presents results from the Nytrox ignition testing campaign, focusing on three potential correlations: 1) chamber pressure versus ignition latency, 2) Nytrox storage pressure versus ignition latency, and 3) Ignition power. These discussions are presented in the following subsections

3.3.1. Effect of Chamber Pressure on Nytrox Ignition Latency

Increasing the pressure of reactants boosts reaction rates by concentrating particles, which leads to more frequent molecular collisions and shorter ignition delays [31]. One measure of the motor ignition latency is identified by the time where the chamber pressure crosses over a specified ignition threshold pressure. A second latency measure is calculated by the time where chamber pressure reaches its maximum rate of increase. The latter measure is determined by numerically differentiating chamber pressure using a time-symmetrical Finite Impulse response (FIR, [32]) filter, which ensures no added latency. Peaks in this curve indicate the maximum rate.

Figure 11 shows time histories for injector feed pressure (a) and chamber pressure (b) during 14 Nytrox-only ignition tests, all synchronized to when injector feed pressure first responds to Nytrox flow. Figure 11(b) marks an assumed 65 psia ignition threshold and highlights when chamber pressure exceeds this value. Figure 11(c) plots the threshold cross-over and peak-rate latency times against steady-state chamber pressure, with second order curve fits shown as dashed black (cross-over), red (peak-rate), and blue (combined latency measures) lines. Figure 11(d) shows the chamber pressure where the maximum rate of change occurs, along with the threshold value.

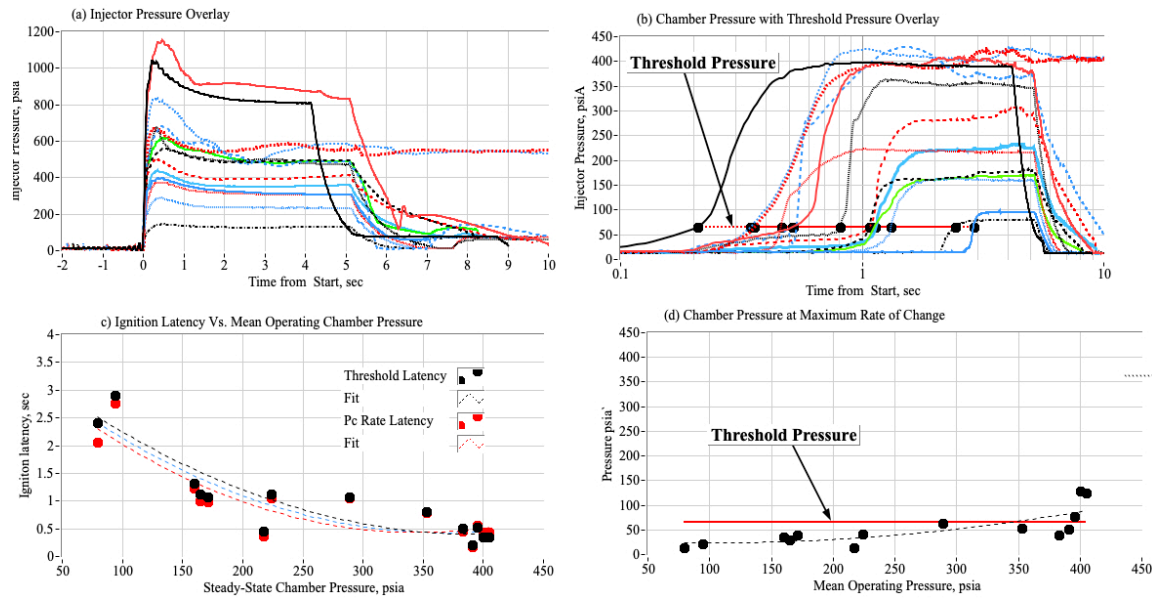


Figure 11. Two Ignition Latency Measures, Plotted as Function of Steady-State Chamber Pressure.

The two latency measures are consistent within 5% and correlate well with steady state chamber pressure. However, the peak rate pressure (black symbols, dashed black line) generally read low when compared to the (arbitrarily assumed) 65 psia ignition threshold pressure. Thus, it is concluded that the assumed threshold pressure is too high.

3.3.2. Estimating the Most Likely Ignition Threshold Pressure

Based on the Data from Figure 11(c) a student's-t statistical analysis used to estimate the probably value for the ignition pressure threshold. The student's t-test assesses (Beckwith et al., 2006, [33]) whether any observed differences between the two data groups--the range of possible ignition threshold values and the observed chamber pressures at maximum rise rate--are statistically significant or simply due to random chance, considering the sample means, variances, and sizes. The corresponding t-value is calculated using Equation (1),

$$t = \frac{|\mu_{threshold} - \mu_{MaxP}|}{\sqrt{\left(\frac{\sigma_{threshold}^2}{n_{threshold}}\right) - \left(\frac{\sigma_{MaxP}^2}{n_{MaxP}}\right)}}, \quad (1)$$

and associated degrees of freedom for the collected data set are approximated by Eq. (2),

$$D.O.F = \frac{\left\{ \left(\frac{\sigma_{threshold}^2}{n_{threshold}} \right) - \left(\frac{\sigma_{MaxP}^2}{n_{MaxP}} \right) \right\}^2}{\left\{ \frac{\left(\frac{\sigma_{threshold}^2}{n_{threshold}} \right)^2}{n_{threshold} - 1} \right\} + \left\{ \frac{\left(\frac{\sigma_{MaxP}^2}{n_{MaxP}} \right)^2}{n_{MaxP} - 1} \right\}}. \quad (2)$$

In Eqs. (1) and (2) the parameters $\{\mu_{threshold}, \sigma_{threshold}, \text{ and } n_{threshold}\}$ represent the statistics associated with the threshold pressure values. For this analysis a series of threshold pressures will be assumed starting at 30 psia and increasing to 100 psia in 5 psia increments, for a total set size with $n_{threshold} = 15$ members. The standard deviation for each member assumed element is assumed to be 5 psia. The parameters $\{\mu_{MaxP}, \sigma_{MaxP}, \text{ and } n_{MaxP}\}$ result from the sample statistics of the data set plotted as the black symbols on Figure 11(b). The pressure at max rate data set contains $n_{MaxP} = 14$ members. For each assigned value of $P_{threshold}$ the t-statistic is calculated and plotted as a function of the $P_{threshold}$.

Figure 12 illustrates the outcome of this calculation. For the two data sets, which together contain 29 members, Equation 2 yields 15 degrees of freedom; the associated critical t-value at the 95% confidence level is roughly 2.147. The raw values from the *MaxP* data set are displayed as black markers, while a dashed black line shows the polynomial fit to the data. Additionally, the critical t-value appears in Figure 12 as a dashed red line. Pressures outside 31–73 psia yield t-statistics above the critical value, indicating they're unlikely ignition thresholds. The t-statistic suggests the most probable threshold is around 52.3 psia. Because the breakpoints only increase by 5 psia increments, their resolution is limited. The optimal threshold pressure is calculated by averaging the pressures corresponding to the two lowest t-scores, with each value weighted according to its t-score,

$$\widehat{P}_{threshold} = \frac{t_1 \cdot P_1 + t_2 \cdot P_2}{t_1 + t_2} \quad (3)$$

Figure 13 re-plots the ignition latency data and threshold pressure data from Figure 11(a), (b), along with a plot of the student's-t probability density function for 15 degrees of freedom. Figure 12(c) also shows that the blue symbol—representing the t-statistics—remains well within the critical range indicated by the dashed red lines. The correlations now demonstrate exceptional alignment. As illustrated in Figure 13(e), the t-Statistic associated with $P_{max} = 52.3$ psia is positioned near the peak of the probability density curve. This value is approximately double the ignition pressure threshold reported by Whitmore et al. (2020, 8) for GOX/Nytxox arc ignition. Their preliminary analysis indicated that the required pressure threshold was about two atmospheres of partial pressure for O_2 concentration. Since gaseous oxygen (O_2) has double the oxygen atoms per mole compared to nitrous oxide (N_2O), this result is expected. Figures 13(a) and 13(b) show, as blue symbols, the ignition latency and pressure of maximum rise for the GOX prelead test. Although these values appear low compared to other data, the ignition latency matches results from Ref. [9], which found a typical ignition latency of about 1/8 seconds in their GOX/ABS tests.

The latency plots presented in Figure 13(a) provide valuable insights for engineers considering Nytxox/ABS thrusters employing a variant of the PRL arc ignition system. When the design chamber pressure is below 200 psia, ignition latency is considerable, exceeding 1000 milliseconds. As chamber pressure increases above 250 psia, latency decreases markedly, stabilizing between 400 and 500 milliseconds. To maximize ignition reliability, it is advisable to maintain chamber pressures above this threshold and adjust throat area as needed to achieve specific thrust and mass flow targets.

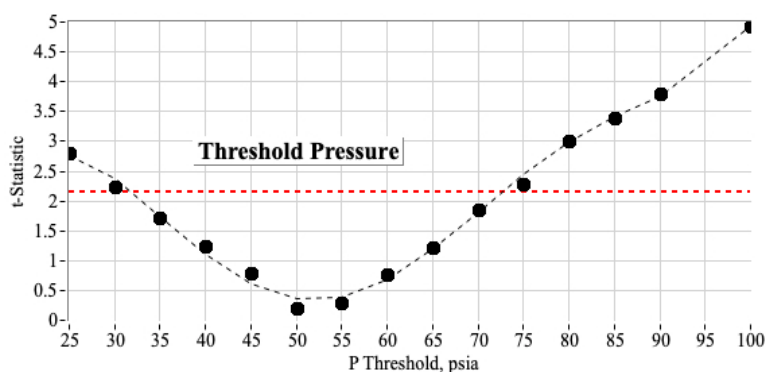


Figure 12. Plotting the t-Statistic for Each of 15 Different Assumed Threshold Pressure Levels.

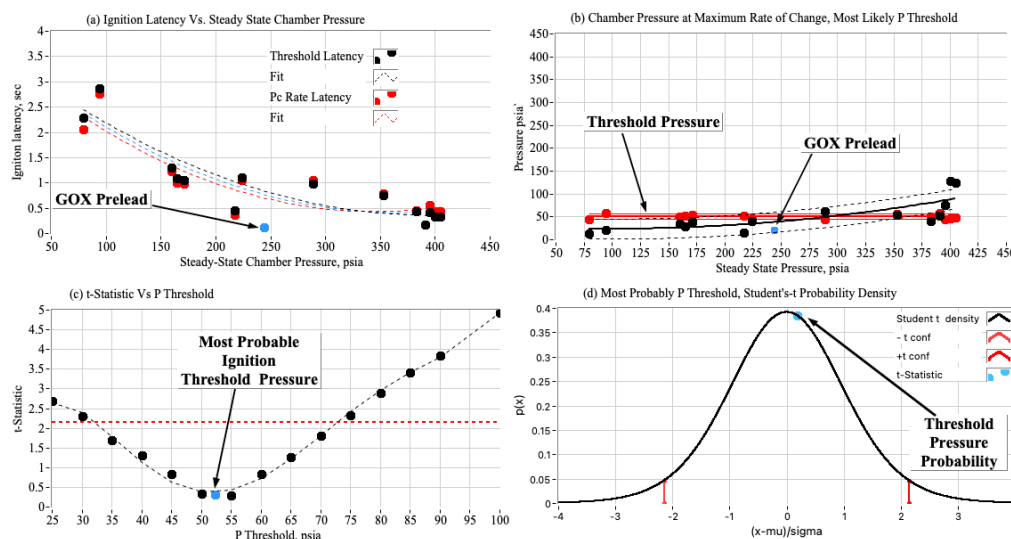


Figure 13. Ignition Latency Threshold Data Replotted Using Most Probable Value Threshold Pressure.

3.3.3. Effect of Nitrox Storage Pressure on Ignition Latency

The second correlation between ignition latency and nitrox storage pressure is less obvious. Ignition latency depends on storage pressure because of the concentration of GOX dissolved in the nitrox mixture. Figure 14 illustrates this relationship: Figure 14(a) displays the O_2 mass fraction in the Nitrox solution for both vapor and liquid states, while Figure 14(b) shows the respective densities of these phases. Both graphs use a storage temperature of 0°C . Within the pressure range of 1250–1450 psig (8720–9650 kPa), the oxygen content in the vapor phase reaches about 45%, which allows for optimal vapor dilution and the highest liquid density.

When storage pressures exceed roughly 105 atmospheres (1560 psig, 10,700 kPa), the proportion of N_2O vapor drops sharply, and the density of the liquid phase decreases. This density drop happens because nitrous oxide and oxygen dissolve into each other, leading to lower density as the oxygen concentration in solution grows. Therefore, keeping storage pressure close to the optimal value—between 85 and 100 atmospheres—is essential for achieving volumetric efficiency with Nitrox. Operating within the storage pressure range from 1250–1450 psig ensures dissolved gaseous oxygen stays between 16% and 20%. These increased oxygen levels boost ignition by raising the local O_2 partial pressure as oxygen escapes during injection.

Analysis of the data presented in Figure 14 indicates that the pressure necessary to maintain oxygen (O_2) in solution significantly exceeds the natural vapor pressure of nitrous oxide (N_2O), which is approximately 440 psia (3040 kPa) at 0°C . Consequently, as the Nitrox mixture passes through the injector into the combustion chamber, oxygen is released from solution, and the resulting boiling mixture facilitates enhanced mechanical mixing and atomization of N_2O droplets within the Nitrox stream. This process achieves improved mixing without the need for additional mechanical devices such as atomizing injectors or spray heads.

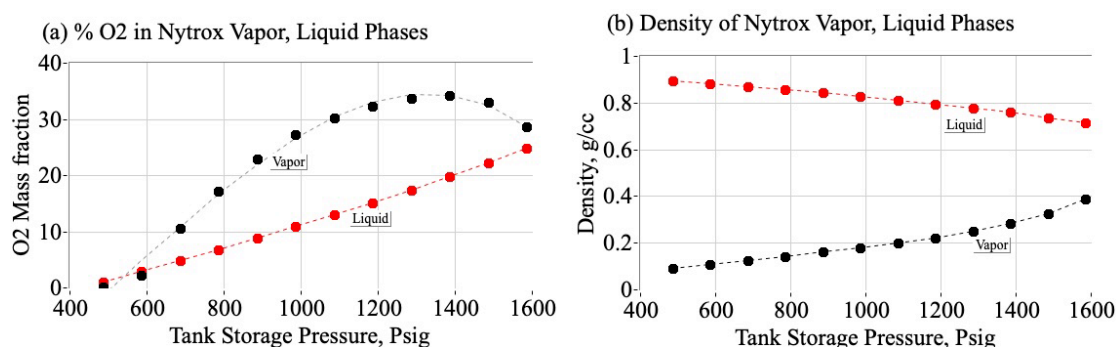


Figure 14. O_2 Mass fraction and Density of Vapor and Liquid Phases of Nytrox as a Function Tank Storage Pressure at 0 °C.

The calculation of Figure 14 was performed using the Peng-Robinson equation of state (1976, Ref. [34]) for a binary two-phase mixture. To combine the O_2 and N_2O binary components, the mixing rule follows the model proposed by Zudkevitch and Joffe (1970, [35]). The numerical algorithm utilized for these calculations adheres to Karabeyoglu's procedure (Ref. 18). At phase equilibrium, the fugacity values for both the liquid and vapor phases of each fluid component are equal. In this context, fugacity is defined as a measure of a mixture component's "tendency to escape" from solution; it matches the pressure of an ideal gas possessing the same Gibbs free energy as the real gas at identical temperatures.

Figure 15 show the correlation of ignition latency to the oxidizer tank storage pressure for the 14 Nytrox-only tests. Figure 15(a) shows tank storage pressure histories for each Nytrox ignition test, and Figure 15(b) displays ignition latencies (from threshold crossover and maximum chamber pressure rate) as functions of mean tank storage pressure for each run. While correlations are weaker than those for chamber pressure (Figure 13a), the comparisons between latencies from crossover pressure and maximum rate of pressure change remain significant and consistent. Therefore, it is likely that Nytrox tank storage pressure affects ignition latency by influencing dissolved O_2 levels.

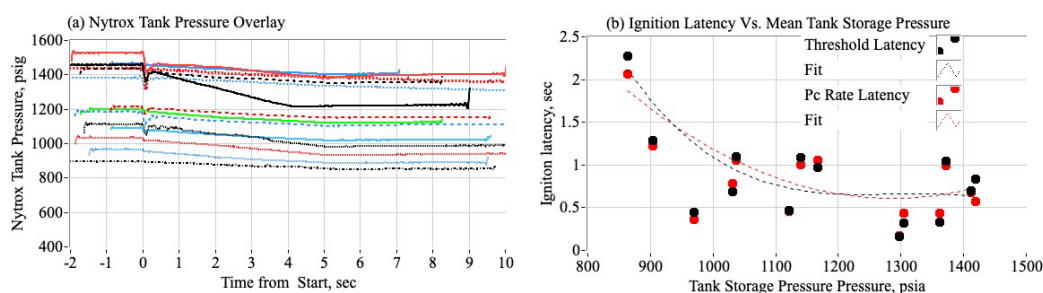


Figure 15. Effect of Tank Storage Pressure on Nytrox Ignition Latency.

3.3.4. Effect of HVPS Ignition Power on Ignition Latency

The final correlation to be examined relates to the power levels consumed by the spark cap during ignition. As outlined in Section 2.1.2, the HPVS system is limited to a total power output of 30 watts. Because the power unit is current-limited, the output current during a typical ignition saturates at 30 milliamps. The voltage supplied to the spark cap depends on the impedance of the arc-path through the ABS material, which generally varies between 2 and 8 kOhms. Figure 16 shows a typical ignition sequence from a 20-second Nytrox-only test, plotting ignition voltage, current, power, total spark energy, and path impedance. Power across the arc path is under 5 watts, total spark energy is approximately 15 joules, and arc-path impedance is about 5 kOhms. Figure 16(b) also overlays chamber pressure on the HVPS current plot. It is important to note the one-second spark pre-lead before the run valve opens.

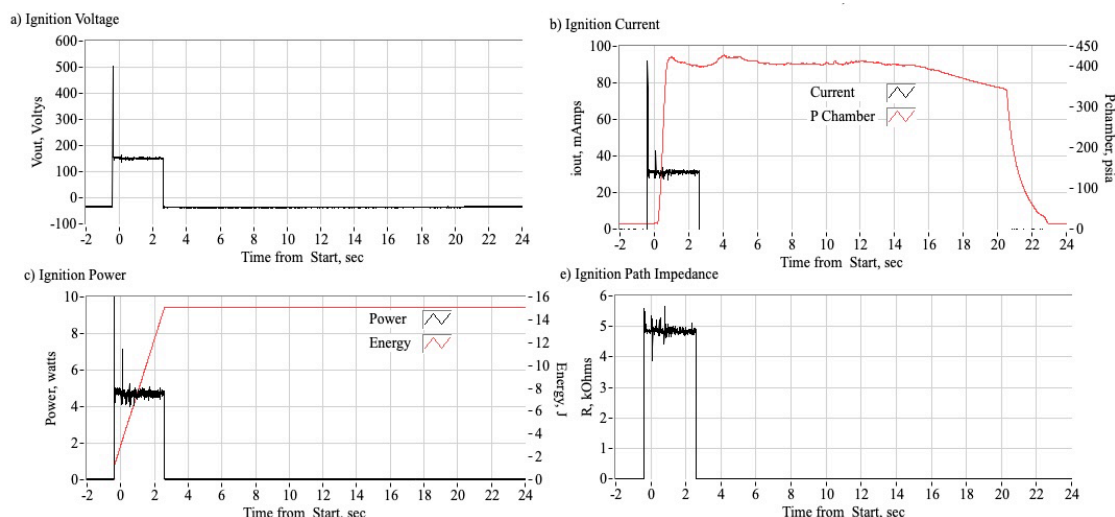


Figure 16. Typical Start Sequence for the Nytrox Ignition Tests.

Figure 17, which plots the ignition latencies against the mean ignition power, shows that ignition latencies from both crossover and maximum pressure analyses have little to no correlation with mean ignition power. For this 30-Watt HVPS data set, ignition power appears to have minimal effect on ignition latency. While a significantly higher power HVPS might reduce latency, it is unsuitable for applications like SmallSats with tight power constraints.

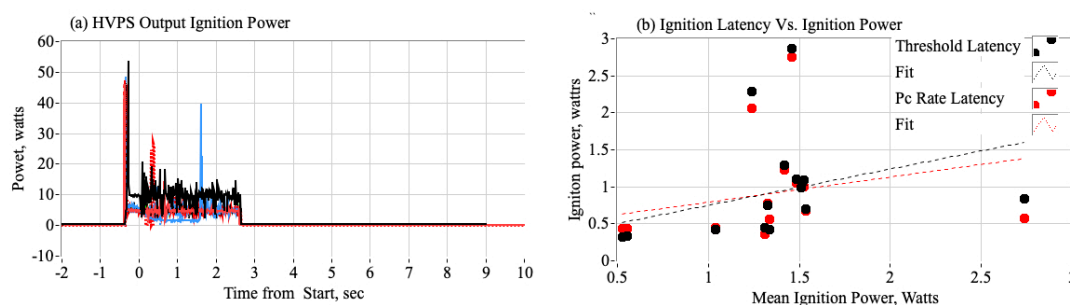


Figure 17. Effect of 30-Watt HVPS Power Output on Nytrox Ignition Latency.

4. Discussion

Previously, it was demonstrated that the ignition delay for the Nytrox/ABS hybrid motor is primarily influenced by the average chamber pressure and, to a lesser extent, by the storage pressure within the Nytrox tank. This research concentrated on examining how storage pressure impacts the amount of dissolved oxygen in the mixture, without addressing temperature effects. However, as will be discussed further, fluctuations in tank temperature during testing can significantly impact the characteristics of the stored Nytrox.

The PRLK's test infrastructure current lacks resources to actively control the Nytrox run tank temperature during testing. Previous ignition tests used an ice bath to keep tanks near 0 °C, but this method was inconvenient and evaporation caused unknown errors in time mass measurements. As described previously in Section 2.2, once the Nytrox run tank is filled, it is stored at -15 °C using a portable industrial-grade freezer. When the tank is removed from the freezer for testing, over time it gradually warms up to room temperature. As will be shown in the upcoming paragraphs, when the tank warms, oxygen shifts from being dissolved in the liquid Nytrox to forming a vapor in the ullage above the liquid. Since the NOS® run tank uses a dip tube that draws liquid Nytrox from the bottom, the drawn liquid will have a significantly lower concentration of oxygen, than when it was first taken from the freezer.

From the original Peng-Robinson [34] analysis presented by Ref. 22, given an initial tank pressure P_{init} at a temperature of T_{init} (prior to warming), the final tank pressure (P_{final}) at the equilibrium test temperature (T_{final}) is

$$P_{final} = \left(\frac{T_{final}}{T_{init}} \right) \cdot \frac{\left(\frac{1}{Z_v} + \frac{1}{Z_l} \right)_{init}}{\left(\frac{1}{Z_v} + \frac{1}{Z_l} \right)_{final}} \cdot P_{init} \quad (4)$$

In Eq. (2), Z is the fluid's compressibility factor, with indices "l" and "v" for liquid and vapor phases. The phase-equilibrium pressure is given by the state vector $\{P, T, Z_v, Z_l\}$ whose values are consistent with the Peng-Robinson model. Figure 18 presents a numerical solution of the Peng-Robinson model, assuming a starting pressure of 62 atms (910 psia, 6280) kPa and an initial temperature of -15°C (the *Nyrox* storage temperature); then warming the solution temperature to 35°C , just below the critical temperature (36.5°C) of nitrous oxide. Figures 17(a)-(c) show the relationship between *Nyrox* phase-equilibrium pressure, O_2 mass concentrations, temperature, and pressure. As the tank warms, pressure increases from 68 atmospheres at 0°C to about 79 atmospheres at 25°C . Figure 17(c) demonstrates that increasing temperature leads to a decrease in dissolved oxygen mass, with O_2 concentrations dropping quickly as the solution heats up, unlike the constant temperature scenario in Figure 14.

As oxygen leaves solution, a stratified mixture forms, separating into layers of O_2 and N_2O vapor; oxygen, being lighter, collects at the top of the tank. If the tank warms sufficiently, the liquid drawn from the bottom dip tube contains little O_2 , and almost no oxygen reaches the injector during ignition, undermining many advantages noted in Section 3.1.1. Therefore, controlling tank temperature is crucial for flight applications. The combined effects of simultaneous *Nyrox* temperature and pressure changes remain insufficiently studied and warrant further investigation.

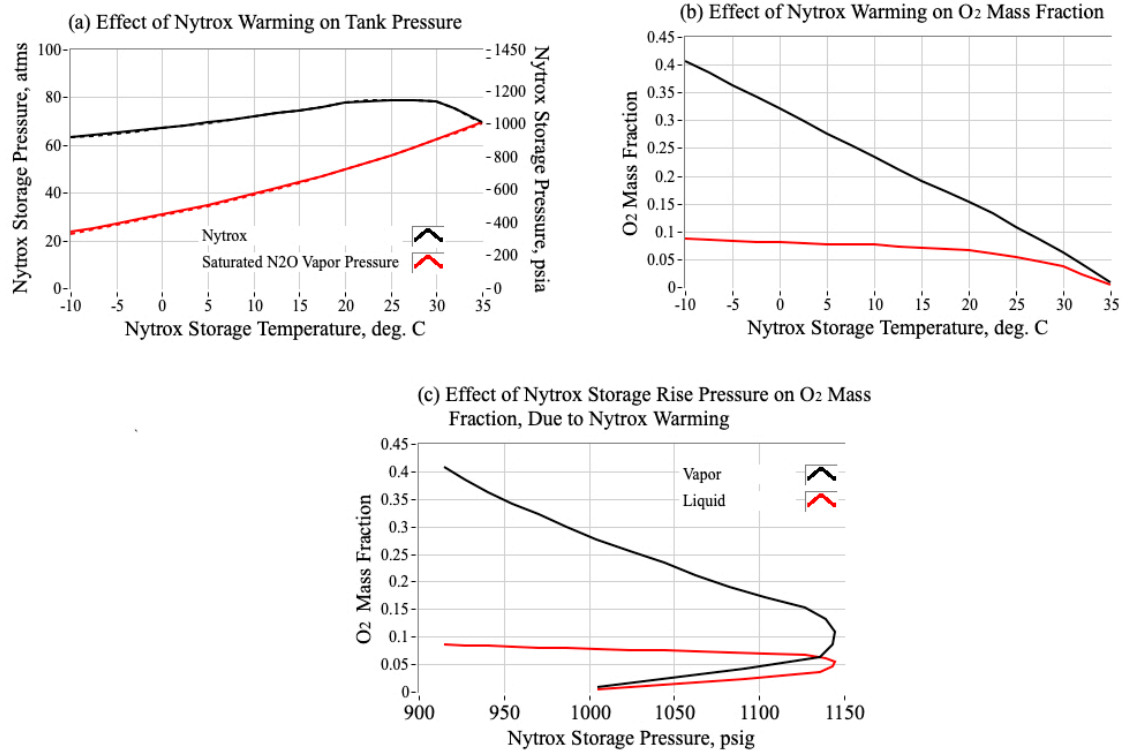


Figure 18. Effect of Warming *Nyrox* on Tank Pressure and O_2 Mass in Solution.

5. Conclusions

Over the last ten years, a new High-Performance "Green" Hybrid Propulsion (HPGHP) system has been developed as an environmentally friendly alternative to hydrazine and other toxic

spacecraft propellants. Previous test and evaluation campaigns have shown that Nytrox, and binary, two-phase blend of nitrous oxide and gaseous oxygen, functions well as high-density oxidizer in HPGHP system. Reported vacuum specific impulse values exceed 300 seconds—substantially higher than what hydrazine-based propellants can achieve.

Historically, hybrid rockets were not considered practical for in-space propulsion, mainly due to the lack of a reliable, reusable ignition system that did not rely on pyrotechnics. This challenge has now been addressed by exploiting the unique electrical breakdown behaviour of ABS thermoplastic produced via fused deposition manufacturing. Additive manufacturing alters these electrical properties so that, when exposed to a high-voltage, low-current electrostatic field, arc-tracking occurs along the printed layers, causing the material to pyrolyze and initiate combustion once an oxidizing agent is present. The engineered system offers high reliability, with the only constraint on restarts being the available fuel. Most startup sequences use 5-15 joules of energy, and after initial ignition, the rocket can be repeatedly fired without needing extra energy input.

A key challenge in utilizing Nytrox as a hybrid oxidizer involves low ignition reliability resulting from high cold-start ignition latency when employing the arc-ignition system. Mitigating ignition latency is critical for the operational viability of the Nytrox HPGHP system, which represents a technology with considerable market potential. This paper details the outcomes of subsequent testing and development initiatives aimed at addressing these concerns. The study concludes that the mean operating chamber pressure has a strong influence on observed ignition delays, and, to a lesser extent, the Nytrox tank storage pressure also influences ignition latency.

Engineers using Nytrox/ABS thrusters with a PRL arc ignition system should note that ignition latency is high (over 1000 ms) below 200 psia chamber pressure but drops to under 500 ms above 250 psia. For reliable ignition, keep chamber pressure above 250 psia and adjust throat area for desired thrust and mass flow.

This research campaign examined how storage pressure at constant temperature influences dissolved oxygen, ignitability, and motor performance. While tank warming effects were not directly studied, post-test analysis revealed that temperature fluctuations can adversely affect Nytrox properties, underscoring the importance of managing tank temperature in flight applications. Further research is recommended on the combined effects of simultaneous temperature and pressure changes during operations and testing.

6. Patents

Whitmore, S. A., Bulcher, A. M., Lewis, Z., and Inkley, N., "Methods and Systems for Restartable Hybrid Rockets," *US Patent 10,774,789 B2*, Sept. 15, 2020. <https://patents.google.com/patent/US20150322892A1/en>, (accessed on 02 March 2026).

Author Contributions: All listed authors contributed significantly to this research project. Conceptualization and methodology, Stephen A. Whitmore 60%, Ryan J. Thibaudeau 25%, Jared S. Coen15%; analysis software, Stephen A. Whitmore 70%, Ryan J. Thibaudeau 20%, Jared S. Coen10%; validation, Stephen A. Whitmore 70%, Ryan J. Thibaudeau 20%, Jared S. Coen10%; formal analysis, Stephen A. Whitmore 50%, Ryan J. Thibaudeau 25%, Jared S. Coen25%; data curation Stephen A. Whitmore 50%, Ryan J. Thibaudeau 25%, Jared S. Coen25%, X.X.; writing—original Stephen A. Whitmore 100%; writing—review and editing, Stephen A. Whitmore 70%, Ryan J. Thibaudeau 20%, Jared S. Coen10%, visualization, Stephen A. Whitmore 100%; supervision, Stephen A. Whitmore 100%; project administration, Stephen A. Whitmore 100%; funding acquisition, Stephen A. Whitmore 100%. All authors have read and agreed to the published version of the manuscript.

Funding: The authors would like to thank the NASA Small Spacecraft Technology Program (SSTP) for partially funding this work through cooperative agreement number 80NSSC20M0083.

Institutional Review Board Statement: N/A.

Informed Consent Statement: N/A.

Data Availability Statement: The data supporting this report are properties of Utah State University. Parties interested in using any of the published test results may request formal data sets by contacting the corresponding author on this report. The authors would like to thank the Utah State University Office of Research and the Vice-President of Research for partially funding this work under the Research Catalyst (RC) program. This work is published under the Fundamental Research Exclusion (FRE) [36] which allows general scientific, mathematical, or engineering principles commonly taught in schools, colleges, and universities, or information in the public domain, to be published without specific US government authorization.

Conflicts of Interest: "The authors declare no conflicts of interest."

Nomenclature

Symbols

N_2O	=	Chemical formula of nitrous oxide
n	=	Number of members in data set
n_{MaxP}	=	Number of samples in max rate data set
$n_{threshold}$	=	Number of threshold pressure data samples
O_2	=	Chemical formula of molecular oxygen
P	=	Pressure, <i>kPa</i>
P_c	=	Combustion (chamber) pressure, <i>kPa</i>
P_{max}	=	Most probably ignition threshold pressure, <i>psia</i>
$P_{threshold}$	=	Threshold pressure for Nitrox Ignition, <i>psia</i>
t	=	Numerical statistic used for student's-t hypothesis test
Z	=	Compressibility of a gas or fluid
μ	=	Sample mean
σ	=	Sample standard deviation

Acronyms and Abbreviations

<i>ABS</i>	=	Acrylonitrile butadiene styrene
<i>BLAST</i>	=	Ballistics and Survivability Limits Testing (Laboratory)
<i>CEA</i>	=	Chemical Equilibrium with Applications, computer program.
<i>D.O.F.</i>	=	Degrees of freedom
<i>FDM</i>	=	Fused deposition modeling
<i>GOX</i>	=	Gaseous oxygen
<i>HPGHP</i>	=	High-Performance Green Hybrid Propulsion
<i>NOS</i> [®]	=	Nitrous Oxide Systems trade name
<i>OSHA</i>	=	Occupational Safety and Health Administration
<i>RMS</i>	=	Root mean squared statistic
<i>TRL</i>	=	Technology readiness level

References

1. Anon., "Hazard Analysis of Commercial Space Transportation; Vol. 1: Operations, Vol. 2: Hazards, Vol. 3: Risk Analysis," *U.S. Dept. of Transportation*, PB93-199040, Accession No. 00620693, May 1988. https://www.faa.gov/about/office_org/headquarters_offices/ast/licenses_permits/media/hazard.pdf, (accessed on 4 March 2026).
2. Anon., "Department of Defense Interface Standard, Eletromagnetic Environmental Effects requirements for Systems, *MIL-STD-464*, March, 1997. <http://www.tscm.com/MIL-STD-464.pdf>, (accessed on 4 March 2026).
3. Palermo, E. Fused Deposition Modeling: Most Common 3D Printing Method. *LIVESCIENCE*, 19 September 2013, Available online: <https://www.livescience.com/39810-fused-deposition-modeling.html>, (accessed on 02 March 2026).

4. Stephen A. Whitmore, Stephen L. Merkley, Louis Tonc, and Spencer D. Mathias, "Survey of Selected Additively Manufactured Propellants for Arc Ignition of Hybrid Rockets", *J. Propulsion and Power*, Vol. 32, No. 6, 2016, pp. 1494-1504. <http://dx.doi.org/10.2514/1.B36106>, (accessed on 02 March 2026).
5. Whitmore, S. A., Mathias, S. D., and Harvey, R., "High Voltage Breakdown and Arc-Tracking Mechanism of Thermoplastics with Applications to Hybrid Rocket Arc- Ignition," *53rd AIAA/SAE/ASEE Joint Propulsion Conference*, 10-12 July 2017, Atlanta, GA. AIAA 2017-4601. <https://doi.org/10.2514/6.2017-4601>, (accessed on 02 March 2026).
6. Hastings, J. K., Zuercher, J. C., Hetzmanseder, E., "Electrical Arcing and Material Ignition Levels," *SAE 2004 World Congress & Exhibition*, March 08, 004, ISSN: 0148-7191, e-ISSN: 2688-3627. <https://doi.org/10.4271/2004-01-1565>, (accessed on 02 March 2026).
7. Jiang, H. Q., Brazis, P. W., Navarro, N, "DC high-energy arcing ignition (HAI) resistance for polymeric materials: Part I: Consistency and repeatability of DC-HAI system," *2012 IEEE Symposium on Product Compliance Engineering Proceedings*, Schematic Scholar, 2012. <https://doi.org/10.1109/ISPCE.2012.6398287>, (accessed on 02 March 2026).
8. Whitmore, S. A., Bulcher, A. M., Lewis, Z., and Inkley, N., "Methods and Systems for Restartable Hybrid Rockets," *US Patent 10,774,789 B2*, Sept. 15, 2020. <https://patents.google.com/patent/US20150322892A1/en>, (accessed on 02 March 2026).
9. . Whitmore, S. A., and Thibaudeau, R. J., "Development of a GOX/ABS Hybrid-Gas Generator System for the NASA Plume Surface Interaction (PSI) Experimental Campaign," *AIAA 2026-2871, AIAA SCITECH 2026 Forum, Orlando FL*, Jan. 12-16, 2026, <https://arc.aiaa.org/doi/abs/10.2514/6.2026-2871>, (accessed on 25 Feb. 2026)
10. Whitmore, S. A., "Three-Dimensional Printing of "Green" Fuels for Low-Cost Small Spacecraft Propulsion Systems," *J. Spacecraft and Rockets*, Vol. 54, No. 6, 2017, <https://doi.org/10.2514/1.A33782>, (accessed on 4 March 2026).
11. Whitmore, S. A., and Thibaudeau, R. J., "Development of a GOX/ABS Hybrid-Gas Generator System for the NASA Plume Surface Interaction (PSI) Experimental Campaign," *AIAA 2026-2871, AIAA SCITECH 2026 Forum, Orlando FL*, Jan. 12-16, 2026, <https://arc.aiaa.org/doi/abs/10.2514/6.2026-2871>, (accessed on 25 Feb. 2026)
12. Whitmore, S. A., and Bulcher, A. M., "A Green Hybrid Thruster Using Moderately Enriched Compressed Air as the Oxidizer", *AIAA 2018-4841, 2018 Joint Propulsion Conference, AIAA Propulsion and Energy Forum*, <https://doi.org/10.2514/6.2018-4841>, (accessed on 02 March 2026).
13. Anon, Nitrous Oxide, NIST Chemistry WebBook, SRD 69, National Institute of Standards and Technology, U.S. Dept. of Commerce, <https://webbook.nist.gov/cgi/cbook.cgi?ID=10024-97-2>, (accessed on 25 Feb. 2025).
14. Story, G., and Arves, J., Kuo, K. K. (ed.), and Chiaverini M. J. (ed.), "Large-Scale Hybrid Motor Testing," In *Fundamentals of Hybrid Rocket Combustion and Propulsion*, American Institute of Aeronautics and Astronautics, Reston, VA, USA, 2007, pp. 513–552, ISBN (print): 978-1-56347-703-4, eISBN: 978-1-60086-687-6, <https://arc.aiaa.org/doi/10.2514/4.866876>, (accessed on 4 March 2026).
15. Anon., "Occupational Safety and Health Guideline for Nitrous Oxide," *US Department of Labor, Occupational Health and Safety Administration*, March 7, 1996. <https://www.osha.gov/laws-regs/regulations/standardnumber/1910/1910.105>, (accessed on 4 March 2026).
16. Rhodes, G., W., "Investigation of Decomposition Characteristics of Gaseous and Liquid Nitrous Oxide," *Air Force Weapons Laboratory*, Report AD-784 602, Kirtland AFB, New Mexico, July 1974. <https://www.freelists.org/archives/aroCKET/01-2014/pdfEE82jaPU9W.pdf>, (accessed on 4 March 2026).
17. Bracken, A.B., Broughton, G.B., Hill, W., "Equilibria for Mixtures of Oxygen and Nitrous Oxide and Carbon Dioxide and Their Relevance to the Storage of N₂O/O₂ Cylinders for Use in Analgesia," *J. Phys. D, Applied Physics*, Vol. 3, 1970, pp.1747–1758, doi:10.1088/0022-3727/3/11/325, (accessed on 4 March 2026).
18. Karabeyoglu, M., A., "Nitrous Oxide and Oxygen Mixtures (Nytrox) as Oxidizers for Rocket Propulsion Applications", *J. Prop. Power*, Vol. 30, No. 3, 2014, pp. 696-706. <https://doi.org/10.2514/1.B34768>, (accessed on 4 March 2026).

19. Whitmore, S. A., "Nytrox as "Drop-in" Replacement for Gaseous Oxygen in SmallSat Hybrid Propulsion Systems," *Aerospace*, Vol. 7, No. 43, 2020, pp. 1-38. <https://doi.org/10.3390/aerospace7040043>. , (accessed on 4 March 2026).
20. Whitmore, S. A., Stoddard, R.L., "N₂O/O₂ blends safe and volumetrically efficient oxidizers for small spacecraft hybrid propulsion," *Aeronaut. Aerosp. Open Access J.* 2019, Vol.2, No. 3. <https://medcraveonline.com/AAOAJ/AAOAJ-03-00097.pdf>. , (accessed on 4 March 2026).
21. Stoddard, R. L., "Experimental Investigation of N₂O/O₂ Mixtures as Volumetrically Efficient Oxidizers for Small Spacecraft Hybrid Propulsion Systems," Master Deg. Thesis, *Utah State University Digital Commons*, December 2019. <https://digitalcommons.usu.edu/>. , (accessed on 4 March 2026).
22. Whitmore, S. A., and Frischkorn, C. I., "Analyzing and Reducing Ignition Latency of a Nytrox/ABS Hybrid Propulsion System," AIAA 2020-3754, *AIAA Propulsion and Energy 2020 Forum Virtual Conference*, August 24-28, 2020, <https://arc.aiaa.org/doi/abs/10.2514/6.2020-3754>, (accessed on 4 March 2026).
23. Anon, "Full-Cone Spray Nozzle Brass, 1/8 NPT Male, 0.5 gal/min @At 20 PSI, 120 Degree Angle," McMaster-Carr, <https://www.mcmaster.com/32885K131/>, {accessed 4 March 2026}.
24. Whitmore, S. A., and Anthony M. Bulcher, A. M., "Vacuum Test of a Novel Green-Propellant Thruster for Small Spacecraft", AIAA 2017-5044. *53rd AIAA/SAE/ASEE Joint Propulsion Conference, AIAA Propulsion and Energy Forum*, 2017. <https://doi.org/10.2514/6.2017-5044>, (accessed on 4 March 2026).
25. Anon. "ULTRAVOLT C Series High Voltage CAP-Charging Supplies. Advanced Energy, Inc.," <https://www.advancedenergy.com/globalassets/resources-root/data-sheets/ultravolt-c-series-data-sheet.pdf>, (accessed on 4 March 2026).
26. Whitmore, S. A., Babb, R. S., Gardner, T. J., Lloyd, K. P, and Stephens, J. C., "Pyrolytic Graphite and Boron Nitride as Low-Erosion Nozzle Materials for Long-Duration Hybrid Rocket Testing, AIAA 2020-3740, *AIAA Propulsion and Energy 2020 Forum*, August 2020. <https://arc.aiaa.org/doi/abs/10.2514/6.2020-3740>, (accessed on 4 March 2026).
27. Holley, "Nitrous Oxide Systems," <https://www.holley.com/brands/nos/>, (accessed on 4 March 2026).
28. Anderson, J. D., *Modern Compressible Flow*, 3rd Edition, New York: The McGraw Hill Companies, Inc., 2003, Chapter 4, pp. 127-187. ISBN-13: 978-0072424430. <https://libcat.lib.usu.edu/search/i0070016542>
29. Gordon, S., and McBride, B. J., "Computer Program for Calculation of Complex Chemical Equilibrium Compositions and Applications, I. Analysis" National Aeronautics and Space Administration, Cleveland, Ohio, Tech. Rep. NASA RP-1311, 1994, <https://ntrs.nasa.gov/api/citations/19950013764/downloads/19950013764.pdf>, (accessed on 23 Jan. 2026)
30. Gordon, S., and McBride, B. J., "Computer Program for Calculation of Complex Chemical Equilibrium Compositions and Applications, II. User's Manual and Program Description" National Aeronautics and Space Administration, Cleveland, Ohio, Tech. Rep. NASA RP-1311-2, 1994, <https://ntrs.nasa.gov/api/citations/19960044559/downloads/19960044559.pdf>, (accessed on 23 Jan. 2026).
31. Anon. ,"18.6: Factors Affecting Reaction Rate," LibreTexts TM, Chemistry, [https://chem.libretexts.org/Bookshelves/Introductory_Chemistry/Introductory_Chemistry_\(CK-12\)/18%3A_Kinetics/18.06%3A_Factors_Affecting_Reaction_Rate](https://chem.libretexts.org/Bookshelves/Introductory_Chemistry/Introductory_Chemistry_(CK-12)/18%3A_Kinetics/18.06%3A_Factors_Affecting_Reaction_Rate), (Accesses 5 March 2025.)
32. R. K. Otnes, L. Enochson, *Applied Time Series Analysis*, Wiley, New York, 1978, 219–260. <https://doi.org/10.1121/1.383336>, (accessed 5 March 2026)
33. Beckwith, T. G., Marangoni, R. D., and Lienhard V, J. H., *Mechanical Measurements*, 6th Ed., Prentice Hall, 2006, pp.43- 73. ISBN-13: 978-0201847659, ISBN-10: 0201847655, https://archive.org/details/mechanicalmeasur0000beck_q2k3, (accessed 5 March 2026)
34. Peng, D.-Y., and Robinson, D. B., "A New Two Constant Equation of State," *Industrial and Engineering Chemistry Fundamentals*, Vol. 15, No. 1, 1976, pp. 59–64. <https://doi.org/10.1021/i160057a011>, (accessed on 23 Jan. 2026).
35. Zudkevitch, D., and Joffe, J., "Correlation and Prediction of Vapor- Liquid Equilibria with the Redlich-Kwong Equation of State" *AIChE Journal*, Vol. 16, No. 1, 1970, pp. 112–119. <https://doi.org/10.1002/aic.690160122>, (accessed on 23 Jan. 2026).

36. Anon., NATIONAL POLICY ON THE TRANSFER OF SCIENTIFIC, TECHNICAL AND ENGINEERING INFORMATION, National Security Decision Directives (NSDDs), 1985. <https://irp.fas.org/offdocs/nsdd/nsdd-189.htm>. (Accessed 7 Feb. 2026)

Disclaimer/Publisher's Note: The statements, opinions and data contained in all publications are solely those of the individual author(s) and contributor(s) and not of MDPI and/or the editor(s). MDPI and/or the editor(s) disclaim responsibility for any injury to people or property resulting from any ideas, methods, instructions or products referred to in the content.